



RNase A Inhibits Formation of Neutrophil Extracellular Traps in Subarachnoid Hemorrhage

Anton Früh^{1†}, Katharina Tielking^{1†}, Felix Schoknecht¹, Shuheng Liu¹, Ulf C. Schneider¹, Silvia Fischer², Peter Vajkoczy^{1*} and Ran Xu¹

OPEN ACCESS

Edited by:

Jean-Luc Morel,
Centre National de la Recherche
Scientifique (CNRS), France

Reviewed by:

Erik Josef Behringer,
Loma Linda University, United States
Md. A. Hakim,
Loma Linda University, United States
Jose Javier Provencio,
University of Virginia Hospital,
United States

*Correspondence:

Peter Vajkoczy
peter.vajkoczy@charite.de

[†]These authors have contributed
equally to this work

Specialty section:

This article was submitted to
Vascular Physiology,
a section of the journal
Frontiers in Physiology

Received: 13 June 2021

Accepted: 10 August 2021

Published: 16 September 2021

Citation:

Früh A, Tielking K, Schoknecht F,
Liu S, Schneider UC, Fischer S,
Vajkoczy P and Xu R (2021)
RNase A Inhibits Formation of
Neutrophil Extracellular Traps in
Subarachnoid Hemorrhage.
Front. Physiol. 12:724611.
doi: 10.3389/fphys.2021.724611

¹Department of Neurosurgery, Charité – Universitätsmedizin Berlin, Corporate Member of Freie Universität Berlin, Humboldt-Universität zu Berlin, and Berlin Institute of Health, Berlin, Germany, ²Department of Biochemistry, Giessen University, Giessen, Germany

Background: Subarachnoid hemorrhage (SAH) caused by rupture of an intracranial aneurysm, is a life-threatening emergency that is associated with substantial morbidity and mortality. Emerging evidence suggests involvement of the innate immune response in secondary brain injury, and a potential role of neutrophil extracellular traps (NETs) for SAH-associated neuroinflammation. In this study, we investigated the spatiotemporal patterns of NETs in SAH and the potential role of the RNase A (the bovine equivalent to human RNase 1) application on NET burden.

Methods: A total number of $n = 81$ male C57Bl/6 mice were operated utilizing a filament perforation model to induce SAH, and Sham operation was performed for the corresponding control groups. To confirm the bleeding and exclude stroke and intracerebral hemorrhage, the animals received MRI after 24 h. Mice were treated with intravenous injection of RNase A (42 $\mu\text{g}/\text{kg}$ body weight) or saline solution for the control groups, respectively. Quadruple-immunofluorescence (IF) staining for cell nuclei (DAPI), F-actin (phalloidin), citrullinated H3, and neurons (NeuN) was analyzed by confocal imaging and used to quantify NET abundance in the subarachnoid space (SAS) and brain parenchyma. To quantify NETs in human SAH patients, cerebrospinal spinal fluid (CSF) and blood samples from day 1, 2, 7, and 14 after bleeding onset were analyzed for double-stranded DNA (dsDNA) via Sytox Green.

Results: Neutrophil extracellular traps are released upon subarachnoid hemorrhage in the SAS on the ipsilateral bleeding site 24 h after ictus. Over time, NETs showed progressive increase in the parenchyma on both ipsi- and contralateral site, peaking on day 14 in periventricular localization. In CSF and blood samples of patients with aneurysmal SAH, NETs also increased gradually over time with a peak on day 7. RNase application significantly reduced NET accumulation in basal, cortical, and periventricular areas.

Conclusion: Neutrophil extracellular trap formation following SAH originates in the ipsilateral SAS of the bleeding site and spreads gradually over time to basal, cortical, and periventricular areas in the parenchyma within 14 days. Intravenous RNase application abrogates NET burden significantly in the brain parenchyma, underpinning a potential role in modulation of the innate immune activation after SAH.

Keywords: neutrophil extracellular traps, neutrophils, subarachnoid hemorrhage, hemorrhagic stroke, neuroinflammation, innate immune response, innate immune reaction

INTRODUCTION

Subarachnoid hemorrhage (SAH) caused by rupture of an intracranial aneurysm, is a life-threatening emergency that is associated with substantial morbidity and mortality (Lawton and Vates, 2017; Van Lieshout et al., 2018). Approximately 5% of all strokes are caused by SAH and the incidence is estimated to be nine per 100,000 person years (Etminan et al., 2019). Women are about 1.24 times more likely to be affected by the disease, and the incidence of SAH increases from the age >50 years and is higher in Japan and Finland compared to other industrialized countries (Macdonald and Schweizer, 2017). Around one-third of SAH patients die within the first 30 days after the initial bleeding event (Schertz et al., 2016). Among survivors, secondary brain injury is described as the main cause of morbidity (Macdonald, 2014). Thereby, emerging evidence points toward involvement of inflammatory processes (Gris et al., 2019), particularly of innate immune cells (Schneider et al., 2015; Lucke-Wold et al., 2016; Zhang et al., 2020).

Among these immune reactions, recent studies suggest that neutrophils play a particular role in SAH induced inflammation (Atangana et al., 2017). Neutrophil granulocytes are the first line of the innate immune system to fight pathogens (Borregaard, 2010). During infectious processes, they exit blood vessel systems, migrate to the site of infection and accumulate in high numbers (Niemic et al., 2015). Neutrophil infiltration into damaged brain tissues has been shown after SAH, stroke, and traumatic brain injury (Liu et al., 2018; García-Culebras et al., 2019; Zeng et al., 2021). Upon stimulation, neutrophils release DNA, granule proteins, and histones (Brinkmann et al., 2004). These fibrillar matrixes are coined as neutrophil extracellular traps (NETs). NETs are involved in various immune reactions and the pathophysiology of diverse diseases (Papayannopoulos, 2018), including central nervous system pathologies (Zhang et al., 2020). The impact of NET formation in SAH has not yet been studied extensively, but recent evidence suggests that they may promote aneurysm rupture, and pharmacological removal of NETs can reduce the rate of aneurysm rupture (Korai et al., 2021). Moreover, there is growing evidence that NETs aggravate the inflammatory events after SAH, and impair revascularization and increase blood brain barrier (BBB) damage after stroke (Kang et al., 2020).

Next to extracellular DNA, other alarmins or so-called danger-associated molecular pattern (DAMP) signals such as extracellular RNA (exRNA) have been described as a key player in the involvement of central system pathologies, including hemorrhagic stroke (Tielking et al., 2019). In this context, RNase is a natural enzyme involved in the regulation of vascular

homeostasis that can counteract exRNA when applied exogenously (Fischer et al., 2011; Lasch et al., 2020; Preissner et al., 2020). Recent studies have shown that NET-associated RNA is a relevant NET component and its formation can occur also independently of DNA, which opened the hypothetical avenue that RNase A (the bovine equivalent to human RNase1) may also modify NET formation *in vivo* SAH models (Herster et al., 2020). Moreover, preliminary data from our laboratory show that RNase A modulates exRNA accumulation in SAH and the microglia-specific immune reaction after SAH.

In this study, with regard to the migratory characteristics of neutrophils, we investigated the spatial and temporal pattern of NET formation in an *in vivo* model of SAH. We report that NET accumulation begins in the ipsilateral side of bleeding, and spreads over time to the parenchyma on both hemispheres, peaking on day 14 after SAH. To confirm these findings in the human system, we also measured NET burden in cerebrospinal spinal fluid (CSF) and blood samples in SAH patients and show that NET accumulation occurs in both compartments significantly. Furthermore, we report that RNase significantly reduces NET formation in the parenchyma, thus being an attractive mediator for evaluation in subsequent studies.

MATERIALS AND METHODS

Study Approval

The analysis on human samples was approved by the local ethics committee of Charité University Hospital (ethical approval number: EA2/134/18). All patients or their authorized individuals gave written consent to the collection of blood and CSF samples. All animal experiments were approved by the Regional Office for Health and Social Affairs (Landesamt für Gesundheit und Soziales; approval number: TVA 0063/18) and were performed in conformity with the German law of animal protection and the National Institute of Health Guidelines for care and use of laboratory animals.

Human Data

Measurement of NET Surrogate Markers in CSF and Peripheral Blood in SAH Patients

Peripheral blood and CSF samples were collected from patients with aneurysmal SAH on day 1, 2, 7, and 14 after SAH onset. For each time point, 2 ml peripheral blood was drawn using Ethylene Diaminetetraacetic acid (EDTA) tubes, and 2 ml CSF was collected from the initial placement of an extraventricular drain (EVD) at onset of SAH, and then further collected from the existing EVD. Some patients also had additional lumbar

drainage, but in this study only ventricular CSF was used. Blood and CSF samples were immediately placed on ice and spun down twice at 4°C at 500g for 5 min, and supernatant was frozen at -80°C before further analysis. Double-stranded DNA (dsDNA) was quantified in CSF and plasma samples as previously published (Ondracek et al., 2020). In detail, samples were incubated with Sytox Green (Thermo Fisher), a fluorescent dsDNA-binding dye, in a concentration of 1 μM for 5 min. Fluorescence intensities (excitation 480 nm, emission 520 nm) were measured in 96-well microplates using a Tecan Infinite M200 reader. Values were normalized to a standard curve of dsDNA (Lambda DNA, Thermo Fisher).

Animal Experiments

Male C57BL/6-mice were kept at the animal facility at the Neuroscience Research Center at Charité University (NWFZ, Berlin). Their age ranged from 8 to 12 weeks and with a weight range of 18–28 g. Animals underwent SAH operation, and sham operation (as the control condition), and were sacrificed at three different time points (1, 7, and 14 days) after operation. A total number of $n=81$ mice were included in this study.

Mouse Model of Subarachnoid Hemorrhage

Subarachnoid hemorrhage was induced with a filament perforation model as described previously (Schneider et al., 2015). Briefly, mice were anesthetized with an intraperitoneal ketamine/xylazine (70 mg resp. 16 mg/kg body weight) injection and placed in supine position. Starting with a midline neck incision, the carotid artery was exposed and a 5–0 non-absorbable monofilament polypropylene suture inserted into the external carotid artery in a retrograde manner and advanced into the common carotid artery. In a next step, the filament invaginated into the internal carotid artery (ICA) and pushed forward to perforate the intracranial arterial bifurcation. Mice were perfused intracardially with PBS.

MRI

All SAH mice received an MRI 24 h after surgery to confirm the bleeding and animals who had a stroke or intracranial hemorrhage (ICH) were excluded from the experiments (Figure 1A). The 1H magnetic resonance imaging was performed on a PharmaScan 70/16U (Bruker Corporation) with a field strength of 7 Tesla by using the software Paravision 5.1 (Bruker Corporation). During the scans, mice received an O₂/N₂O + isoflurane gas anesthesia. The animals' respiration was observed with Small Animal Monitoring System (SA Instruments, Inc.), while their temperature was maintained *via* controlled warming blankets. The presence of SAH was validated from T2 weighted image. Here, SAH volume was estimated based on the formula $V = (A_1 + A_2 + \dots + A_x) \cdot d$, by which A_n corresponds to the bleeding area on each coronal MRI and d corresponds to the MRI slide thickness.

RNase Treatment

Both groups (Sham and SAH animals) received treatment with RNase A (Thermoscientific EN0531), which was administered intravenously (42 μg/kg body weight) and intravenous application of saline solution was used as a control, as described previously

(Walberer et al., 2009). The first injection was administered perioperatively to ensure penetration to the CNS due to breakdown of the BBB after SAH surgery. Due to anesthesia of mice during operation as well their supine positioning, the first injection was applied *via* the sublingual vein. The further injections were repeated every 3 days in the tail vein until scarification as previously reported (Fischer et al., 2013). The total volume of injection was 100 μl at a flow rate of 20 μl/s.

Preparation of the Subarachnoid Space for Immunohistochemistry

To preserve the SAS, whole skulls were harvested and kept in an ascending concentration series of sucrose for proper dehydration (4 days at 20%, 4 days at 30%, and 4 days at 40%) at 4°C and then snap frozen with isopentane. The skulls were then embedded in Tissue-Tek O.C.T. Compound (4583, Sakura Finetek) and carefully cut into 10 μm thin slices with Microm Sec35 blades (Termo APD Consumables) using a cryostat (Thermo Fisher Scientific Inc. Microm HM 560).

Immunofluorescence

Brain sections were blocked for 30 min with 5% bovine serum albumin (BSA) in Tris-Buffered Saline with 0.05% Tween (TBST) at room temperature. After that, primary antibodies against citrullinated H3 (rabbit, 1:30, ab5103, Abcam), NeuN (rabbit, 1:200, ABN78, Millipore), and F-actin (Alexa Fluor 488 Phalloidin, 1:200, A12379, Thermo Fisher Scientific) diluted in 5% BSA/TBST were added for incubation at 4°C over night. The next day, sections were washed three times in 5% BSA/TBST for 10 min, followed by 1.5 h of incubation with the secondary antibodies Rhodamine Red-X-conjugated Donkey IgG anti-Mouse (1:200, 715-295-151, Dianova) and Alexa Fluor 647-conjugated Donkey IgG anti-Rabbit IgG (1:200, 711-605-152, Dianova), diluted in 5% BSA/TBST. After secondary antibody incubation, specimens were washed three times in PBS for 5 min and mounted with DAPI Mounting Medium (SCR-038448, Dianova). The sections were then imaged with confocal microscopy (Leica DM 6000/SP5) and analyzed with ImageJ. Amount of NETs was determined by calculating the ratio area covered by citH3 over total area covered by phalloidin, NeuN, and DAPI (Supplementary Figure S1).

Statistical Analysis and Figures

Data were analyzed using GraphPad Prism for statistical analyses (Graphpad Software, Version 6.0). ANOVA analyses were used to compare multiple, unpaired *t*-tests for the comparison of two groups. The values are displayed as means ± SEs and values of $p < 0.05$ were considered statistically significant. Elements of Figures 1A, 2A,B, 3A were composed with BioRender.com.

RESULTS

NETs Are Released After Onset of Subarachnoid Bleeding in an *in vivo* Mouse Model of Subarachnoid Hemorrhage

To determine whether NETs are released upon subarachnoid hemorrhage *in vivo*, we utilized a filament perforation model

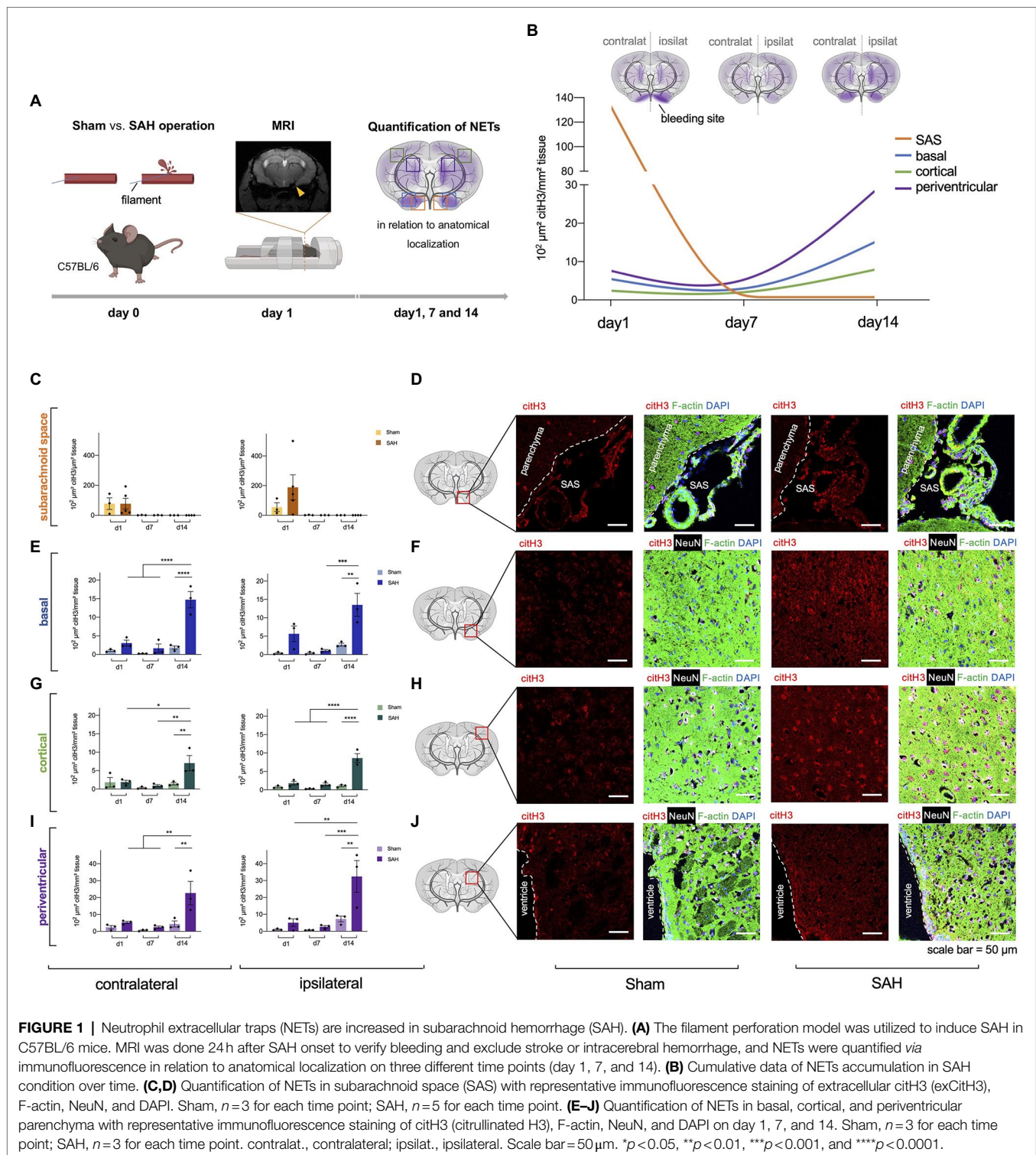


FIGURE 1 | Neutrophil extracellular traps (NETs) are increased in subarachnoid hemorrhage (SAH). **(A)** The filament perforation model was utilized to induce SAH in C57BL/6 mice. MRI was done 24h after SAH onset to verify bleeding and exclude stroke or intracerebral hemorrhage, and NETs were quantified *via* immunofluorescence in relation to anatomical localization on three different time points (day 1, 7, and 14). **(B)** Cumulative data of NETs accumulation in SAH condition over time. **(C,D)** Quantification of NETs in subarachnoid space (SAS) with representative immunofluorescence staining of extracellular citH3 (exCitH3), F-actin, NeuN, and DAPI. Sham, $n=3$ for each time point; SAH, $n=5$ for each time point. **(E–J)** Quantification of NETs in basal, cortical, and periventricular parenchyma with representative immunofluorescence staining of citH3 (citruinated H3), F-actin, NeuN, and DAPI on day 1, 7, and 14. Sham, $n=3$ for each time point; SAH, $n=3$ for each time point. contralat., contralateral; ipsilat., ipsilateral. Scale bar = 50 μm . * $p < 0.05$, ** $p < 0.01$, *** $p < 0.001$, and **** $p < 0.0001$.

to induce subarachnoid hemorrhage in C57BL/6 mice, while Sham operation was performed as a control condition. MRI was conducted 24h after bleeding to verify SAH and exclude other pathologies such as stroke or intracerebral hemorrhage (Figure 1A), and NETs quantified *via* immunofluorescence staining using citrullinated Histone (citH3), a known specific

marker for NET remnants (Wang et al., 2009). Indeed, increased levels of NET formation were found in SAH with the highest amount in the SAS on the ipsilateral side (where bleeding was induced) on day 1 (Figures 1C,D), while after this time point they were essentially not detectable anymore in both control and SAH conditions (Figure 1C). In contrast, in the

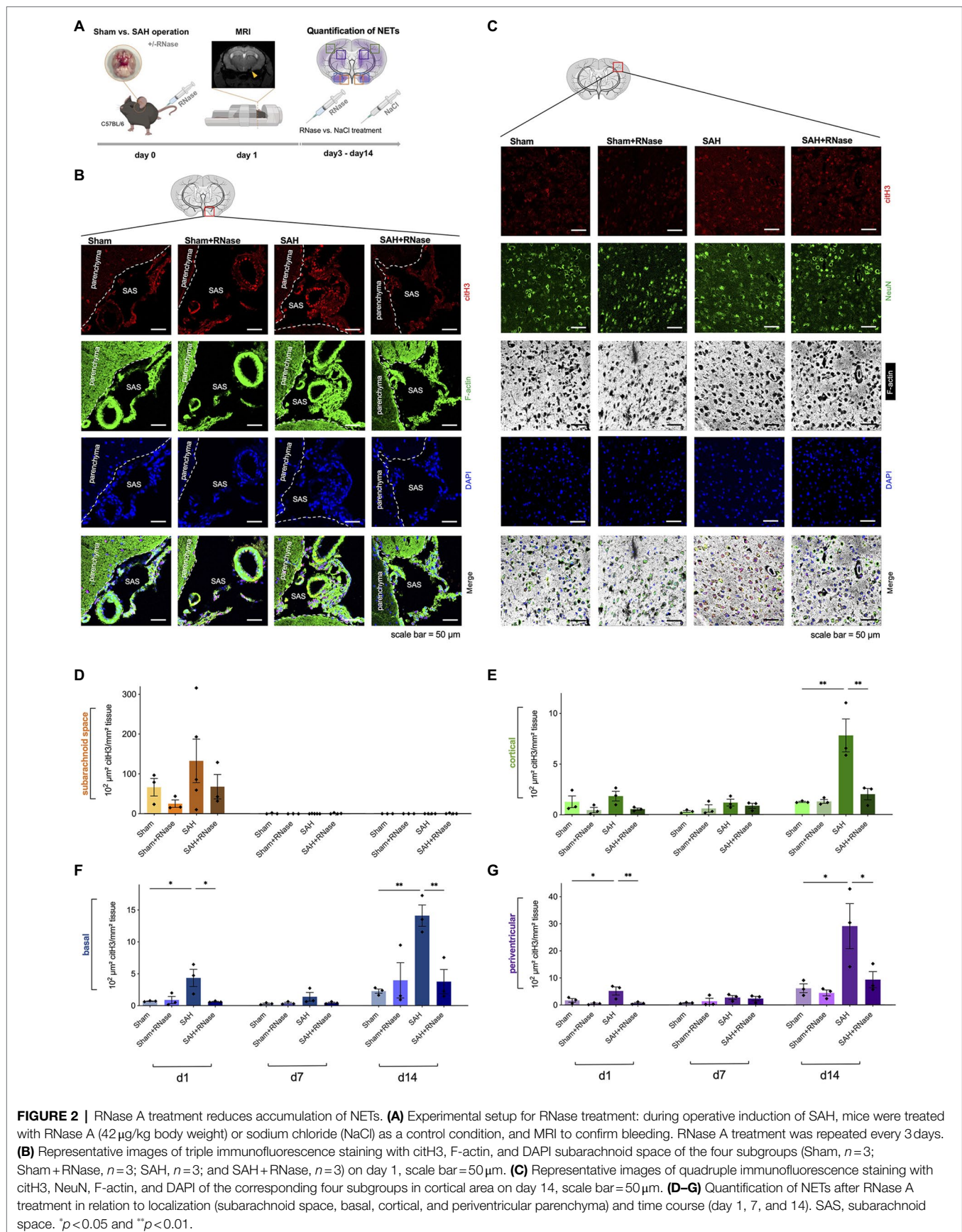
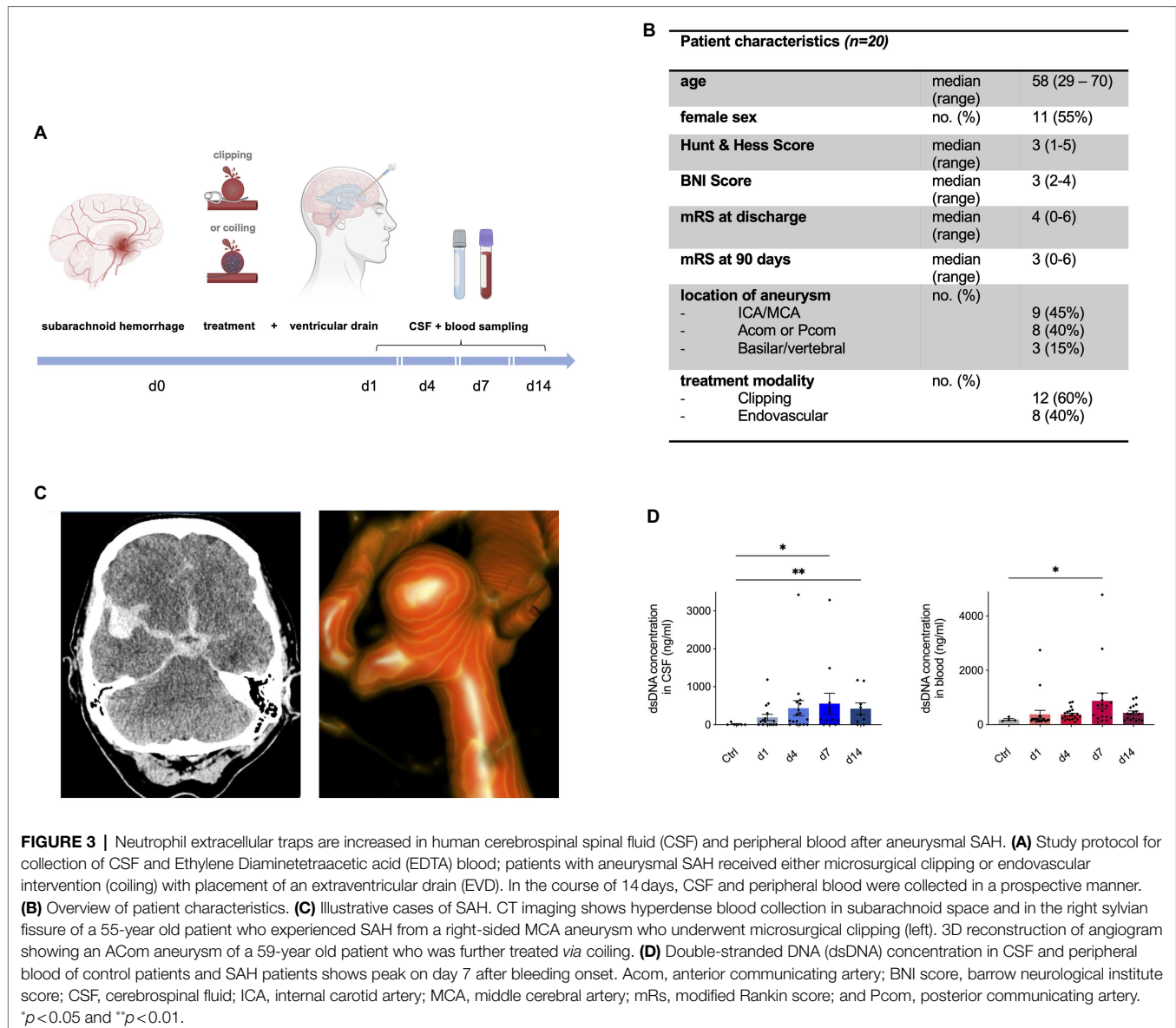


FIGURE 2 | RNase A treatment reduces accumulation of NETs. **(A)** Experimental setup for RNase treatment: during operative induction of SAH, mice were treated with RNase A (42 μ g/kg body weight) or sodium chloride (NaCl) as a control condition, and MRI to confirm bleeding. RNase A treatment was repeated every 3 days. **(B)** Representative images of triple immunofluorescence staining with *citH3*, F-actin, and DAPI subarachnoid space of the four subgroups (Sham, $n = 3$; Sham+RNase, $n = 3$; SAH, $n = 3$; and SAH+RNase, $n = 3$) on day 1, scale bar = 50 μ m. **(C)** Representative images of quadruple immunofluorescence staining with *citH3*, NeuN, F-actin, and DAPI of the corresponding four subgroups in cortical area on day 14, scale bar = 50 μ m. **(D–G)** Quantification of NETs after RNase A treatment in relation to localization (subarachnoid space, basal, cortical, and periventricular parenchyma) and time course (day 1, 7, and 14). SAS, subarachnoid space. * $p < 0.05$ and ** $p < 0.01$.



parenchyma, the NETs showed a gradual increase over time with the highest density on day 14 in all localizations (Figures 1E–J). Interestingly, NET accumulation followed a spreading pattern within the parenchyma from basal to cortical over time, with the most significant increase in periventricular localization (Figure 1B).

Pharmacological Modulation With RNase A Reduces NET Formation

Since recent evidence suggests that NET-associated RNA is a physiologically relevant NET component and its formation can occur also independently of the canonical NET component DNA (Herster et al., 2020), we questioned whether RNase A application can modify NET burden in SAH *in vivo*. RNase A seemed a feasible therapeutic approach since previous studies in our group showed that RNase A can modulate other DAMPs

including exRNA, and influence the microglia-specific immune reaction after SAH. Hence, we treated mice with intravenous application of RNase A and quantified NETs in both SAS and parenchyma (Figure 2A). In SAS, RNase A decreased NET accumulation on day 1, but this was not statistically significant. In contrast, in the parenchyma, RNase A reduced NET accumulation significantly, specifically on day 14, where accumulation of citH3 peaked in all localizations (Figures 2B–G).

NETs Are Increased in Both CSF and Blood of SAH Patients

Next, we questioned whether this observed NET accumulation after SAH is also relevant in the human system. To investigate this, CSF and blood samples were collected within the scope of a prospective observational study in aneurysmal SAH patients (Figure 3A), and NETs were measured *via* quantification of

dsDNA *via* Sytox Green. **Figure 3B** shows the baseline characteristics of the SAH patients included in the study. **Figure 3C** illustrates imaging from two exemplary cases of SAH patients: on the left side, a CT scan of a 55-year old female patient is shown with SAH (Hunt&Hess grade II) with a ruptured right-sided middle cerebral artery (MCA) aneurysm who underwent microsurgical clipping; on the right side, a three-dimensional reconstruction of a ruptured anterior communicating artery (ACom) aneurysm of a 59-year old female (Hunt & Hess grade II) is shown who was further treated with aneurysm coiling. The control patients comprised of patients in which lumbar puncture was done to rule out meningitis or SAH without evidence of any intracranial pathology. Interestingly, dsDNA was significantly increased in both CSF and peripheral blood of SAH patients compared to the control group, with a gradual increase over time, peaking in both compartments on day 7 (**Figure 3D**).

DISCUSSION

Aneurysmal SAH remains a devastating pathology with high morbidity and mortality, and attempts to reduce secondary brain damage have been made for decades, yet the exact pathomechanism contributing to the long-term damage is unclear (Black, 1986; Peterson et al., 1990; Mathiesen et al., 1997; Sheehan et al., 1999). Recent data suggests involvement of the immune system attributable to secondary brain damage, specifically through an outside-in activation of neutrophil recruitment to endothelium, contributing to microglia activation and neuronal apoptosis (Schneider et al., 2015; Atangana et al., 2017). Among the classical immune defense mechanisms of neutrophils, consisting of engulfment of microbes and secretion of anti-microbials, recent data pinpoints to a novel function of neutrophils as part of the innate immune response – the formation of NETs to kill extracellular pathogens (Brinkmann et al., 2004).

In this study, we sought to investigate the potential role of NET formation in SAH and describe the spatiotemporal patterns of NET accumulation after SAH. We demonstrate that in the acute setting, a direct flood of NET formation occurs in the ipsilateral subarachnoid space (SAS), while in the parenchyma, NET levels increase gradually over time in basal, cortical, and periventricular compartments distant to the region of bleeding. These findings are supported by a recent study reporting NET accumulation after SAH as well as their involvement in neuroinflammatory events, albeit the time point of the peak of NETs differed to some degree (Zeng et al., 2021). Interestingly, in the study by Zeng et al. (2021), inhibition of NET formation *via* the PAD4 antagonist GSK484 as well as DNase I inhibited NET-associated neuroinflammation. Our data show that the quantitatively most relevant NET formation occurred 14 days after SAH specifically in periventricular localizations. This is intriguing as it raises the question whether NETs may also be involved in CSF hydrodynamics after aneurysmal SAH, especially since post-hemorrhagic hydrocephalus is a common complication after SAH (Germanwala et al., 2010).

Moreover, while a direct inhibition of NETs *via* DNase has been postulated as a potential mechanistic treatment strategy

to reduce NET burden (Ondracek et al., 2020; Korai et al., 2021), there is mounting evidence that NET-associated RNA is a relevant component of NET formation and can occur independently of DNA (Herster et al., 2020). Based on this finding and previously published data on the dampening effects of RNase A on immune cells (Lasch et al., 2020), we questioned whether RNase A also modifies NET formation. Indeed, our data show that RNase A significantly reduces NET formation in all compartments of the brain. This specific effect on the CNS may be explained by the blood brain barrier breakdown after SAH with permeability to also bigger proteins such as Evans Blue (70kDa; Blecharz-Lang et al., 2018). In our experiments, we used a 13.7kDa pancreatic RNase A for pre- and postoperative intravenous injections. These findings are particularly compelling since RNase therapeutics have already been used to some degree in clinical trials (Mikulski et al., 2002; Ardelit et al., 2007; Chang et al., 2010; Squiquera et al., 2017). Therefore, it is tempting to speculate that RNase may be an accessible interesting potential therapeutic strategy for treatment of the underlying immune reaction after SAH. However, the influence of i.v. application of RNase on physiological processes such as regulation of cerebral blood flow was not investigated in this study and should be addressed in further studies.

The exact molecular mechanisms of NET formation are not fully understood. SAH promotes generation of reactive oxygen species (ROS; Ayer and Zhang, 2008), that have also been described as triggers of NET formation (Erpenbeck and Schön, 2017). Therefore, one may pose the hypothesis that ROS-activation in the setting of SAH contributes NET accumulation, which then may promote microglial activation leading to the activation of neuroinflammatory cascades. Furthermore, recent studies have described that NET formation in the context of SAH increases levels of cytokines such as IL-1 β , IL-6, and TNF- α (Zeng et al., 2021).

Furthermore, in order to investigate whether NET burden is also relevant in the human system, we measured circulating NET abundance *via* the surrogate marker dsDNA and show that increased levels are found in both CSF and peripheral blood of SAH patients. Here, we observed a peak of dsDNA 7 days after the bleeding event, supporting the *in vivo* data from our SAH mouse model. Our findings are in line a recent study of Zeng et al. (2021) showed that a significant increase of citH3 in patients suffering SAH after 24h of the bleeding event, which correlated with the clinical Hunt and Hess score. Additionally, we showed for the first time the further temporal dynamics of NETs and their involvement in CSF in humans. The postponed peak of NET burden potentially indicates a therapeutic window after the bleeding event to attenuate secondary brain damage after SAH. The accumulation of NETs in the brain parenchyma also raises intriguing questions of its origin. Increasing levels of neutrophils in the CSF after SAH have also been associated with development of vasospasms (Provencio et al., 2010). Therefore, neutrophils may migrate in the brain parenchyma after SAH and produce NETs *in situ* as already described in other studies in a model of ischemic stroke (Kang et al., 2020).

Our study is limited by a small sample size, investigations on the association of NET burden and clinical characteristics, and exploratory studies on cell-specific mechanism by which

NETs may affect further inflammatory events in SAH. Albeit the range of the SAH patients in our small study cohort varies between 29 and 70, the median age of our study group in the patients is 58, which is fairly representative of typical age of aneurysm rupture in large cohorts (Rinkel et al., 1998; Shea et al., 2007; Jordan et al., 2009). In order to investigate potential aging effects, further subgroup analyses on young and old mice with larger study numbers are necessary. As we analyzed exclusively male mice, sex-related effects in the animal experiments cannot be excluded. This study also did not investigate the impact of RNase treatment on humans. As potential neuroprotective effects of RNase in SAH patients are of pressing interest, a clinical study on the effect of RNase treatment in hemorrhagic stroke patients are planned for the future.

In summary, our data reveal the spatiotemporal dynamics of NET accumulation after SAH *in vivo* with evidence for a gradual increase of NET formation over time, both in a SAH mouse model as well as in patients suffering aneurysmal SAH. Intriguingly, intravenous RNase A application abrogates NET burden in the parenchyma, underpinning a potential role in of RNase in the innate immune response after SAH. Further studies are needed to fully elucidate the exact nature of NET formation and related immune cell-specific changes of RNase application after SAH.

DATA AVAILABILITY STATEMENT

The raw data supporting the conclusions of this article will be made available by the authors, without undue reservation.

ETHICS STATEMENT

The studies involving human participants were reviewed and approved by Ethikkommission Charité,

REFERENCES

- Ardelt, B., Juan, G., Burfeind, P., Salomon, T., Wu, J. M., Hsieh, T. C., et al. (2007). Onconase, an anti-tumor ribonuclease suppresses intracellular oxidative stress. *Int. J. Oncol.* 31, 663–669. doi: 10.3892/ijo.31.3.663
- Atangana, E., Schneider, U. C., Blecharz, K., Magrini, S., Wagner, J., Nieminen-Kelha, M., et al. (2017). Intravascular inflammation triggers intracerebral activated microglia and contributes to secondary brain injury after experimental subarachnoid hemorrhage (eSAH). *Transl. Stroke Res.* 8, 144–156. doi: 10.1007/s12975-016-0485-3
- Ayer, R., and Zhang, J. (2008). "Oxidative stress in subarachnoid haemorrhage: significance in acute brain injury and vasospasm," in *Cerebral Vasospasm*. ed. T. Kiris (Springer), 33–41.
- Black, P. M. (1986). Hydrocephalus and vasospasm after subarachnoid hemorrhage from ruptured intracranial aneurysms. *Neurosurgery* 18, 12–16. doi: 10.1227/00006123-198601000-00003
- Blecharz-Lang, K. G., Wagner, J., Fries, A., Nieminen-Kelha, M., Rosner, J., Schneider, U. C., et al. (2018). Interleukin 6-mediated endothelial barrier disturbances can be attenuated by blockade of the IL6 receptor expressed in brain microvascular endothelial cells. *Transl. Stroke Res.* 9, 631–642. doi: 10.1007/s12975-018-0614-2

Charité – Universitätsmedizin, Berlin (Germany). The patients/participants provided their written informed consent to participate in this study. The animal study was reviewed and approved by Landesamt für Gesundheit und Soziales (LaGeSo) Berlin (Germany).

AUTHOR CONTRIBUTIONS

KT, FS, AF, SL, and RX conducted the experiments and analyzed the data. RX, AF, and PV designed the study. All authors contributed to the article and approved the submitted version.

FUNDING

RX was supported by the BIH-Charité Clinician Scientist Program funded by the Charité – Universitätsmedizin Berlin and the Berlin Institute of Health. We acknowledge support from the German Research Foundation (DFG) and the Open Access Publication Fund of Charité – Universitätsmedizin Berlin. KT is supported by the Berlin Institute of Health (BIH) Research Stipend as well as the Sonnenfeld Foundation.

ACKNOWLEDGMENTS

This paper is dedicated to the work of our dear colleague and friend Klaus T. Preissner.

SUPPLEMENTARY MATERIAL

The Supplementary Material for this article can be found online at: <https://www.frontiersin.org/articles/10.3389/fphys.2021.724611/full#supplementary-material>

- Borregaard, N. (2010). Neutrophils, from marrow to microbes. *Immunity* 33, 657–670. doi: 10.1016/j.immuni.2010.11.011
- Brinkmann, V., Reichard, U., Goosmann, C., Fauler, B., Uhlemann, Y., Weiss, D. S., et al. (2004). Neutrophil extracellular traps kill bacteria. *Science* 303, 1532–1535. doi: 10.1126/science.1092385
- Chang, C.-H., Gupta, P., Michel, R., Loo, M., Wang, Y., Cardillo, T. M., et al. (2010). Ranpirnase (frog rnase) targeted with a humanized, internalizing, anti-trop-2 antibody has potent cytotoxicity against diverse epithelial cancer cells. *Mol. Cancer Ther.* 9, 2276–2286. doi: 10.1158/1535-7163.MCT-10-0338
- Erpenbeck, L., and Schön, M. (2017). Neutrophil extracellular traps: protagonists of cancer progression? *Oncogene* 36, 2483–2490. doi: 10.1038/onc.2016.406
- Etminan, N., Chang, H.-S., Hackenberg, K., De Rooij, N. K., Vergouwen, M. D., Rinkel, G. J., et al. (2019). Worldwide incidence of aneurysmal subarachnoid hemorrhage according to region, time period, blood pressure, and smoking prevalence in the population: a systematic review and meta-analysis. *JAMA Neurol.* 76, 588–597. doi: 10.1001/jamaneurol.2019.0006
- Fischer, S., Gesierich, S., Griemert, B., Schanzer, A., Acker, T., Augustin, H. G., et al. (2013). Extracellular RNA liberates tumor necrosis factor-alpha to promote tumor cell trafficking and progression. *Cancer Res.* 73, 5080–5089. doi: 10.1158/0008-5472.CAN-12-4657

- Fischer, S., Nishio, M., Dadkhahi, S., Gansler, J., Saffarzadeh, M., Shibamiyama, A., et al. (2011). Expression and localisation of vascular ribonucleases in endothelial cells. *Thromb. Haemost.* 105, 345–355. doi: 10.1160/TH10-06-0345
- García-Culebras, A., Durán-Laforet, V., Peña-Martínez, C., Moraga, A., Ballesteros, I., Cuartero, M. I., et al. (2019). Role of TLR4 (toll-like receptor 4) in N1/N2 neutrophil programming after stroke. *Stroke* 50, 2922–2932. doi: 10.1161/STROKEAHA.119.025085
- Germanwala, A. V., Huang, J., and Tamargo, R. J. (2010). Hydrocephalus after aneurysmal subarachnoid hemorrhage. *Neurosurg. Clin. N. Am.* 21, 263–270. doi: 10.1016/j.nec.2009.10.013
- Gris, T., Laplante, P., Thebault, P., Cayrol, R., Najjar, A., Joannette-Pilon, B., et al. (2019). Innate immunity activation in the early brain injury period following subarachnoid hemorrhage. *J. Neuroinflammation* 16:253. doi: 10.1186/s12974-019-1629-7
- Herster, F., Bittner, Z., Archer, N. K., Dickhofer, S., Eisel, D., Eigenbrod, T., et al. (2020). Neutrophil extracellular trap-associated RNA and LL37 enable self-amplifying inflammation in psoriasis. *Nat. Commun.* 11:105. doi: 10.1038/s41467-019-13756-4
- Jordan, L. C., Johnston, S. C., Wu, Y. W., Sidney, S., and Fullerton, H. J. (2009). The importance of cerebral aneurysms in childhood hemorrhagic stroke: a population-based study. *Stroke* 40, 400–405. doi: 10.1161/STROKEAHA.108.518761
- Kang, L., Yu, H., Yang, X., Zhu, Y., Bai, X., Wang, R., et al. (2020). Neutrophil extracellular traps released by neutrophils impair revascularization and vascular remodeling after stroke. *Nat. Commun.* 11:2488. doi: 10.1038/s41467-020-16191-y
- Korai, M., Purcell, J., Kamio, Y., Mitsui, K., Furukawa, H., Yokosuka, K., et al. (2021). Neutrophil extracellular traps promote the development of intracranial aneurysm rupture. *Hypertension* 77, 2084–2093. doi: 10.1161/HYPERTENSIONAHA.120.16252
- Lasch, M., Kumaraswami, K., Nasicionyte, S., Kircher, S., Van Den Heuvel, D., Meister, S., et al. (2020). RNase A treatment interferes with leukocyte recruitment, neutrophil extracellular trap formation, and angiogenesis in ischemic muscle tissue. *Front. Physiol.* 11:576736. doi: 10.3389/fphys.2020.576736
- Lawton, M. T., and Vates, G. E. (2017). Subarachnoid hemorrhage. *N. Engl. J. Med.* 377, 257–266. doi: 10.1056/NEJMcP1605827
- Liu, Y.-W., Li, S., and Dai, S.-S. (2018). Neutrophils in traumatic brain injury (TBI): friend or foe? *J. Neuroinflammation* 15:146. doi: 10.1186/s12974-018-1173-x
- Lucke-Wold, B. P., Logsdon, A. F., Manoranjan, B., Turner, R. C., McConnell, E., Vates, G. E., et al. (2016). Aneurysmal subarachnoid hemorrhage and neuroinflammation: a comprehensive review. *Int. J. Mol. Sci.* 17:497. doi: 10.3390/ijms17040497
- Macdonald, R. L. (2014). Delayed neurological deterioration after subarachnoid haemorrhage. *Nat. Rev. Neurol.* 10, 44–58. doi: 10.1038/nrneurol.2013.246
- Macdonald, R. L., and Schweizer, T. A. (2017). Spontaneous subarachnoid haemorrhage. *Lancet* 389, 655–666. doi: 10.1016/S0140-6736(16)30668-7
- Mathiesen, T., Edner, G., Ulfarsson, E., and Andersson, B. (1997). Cerebrospinal fluid interleukin-1 receptor antagonist and tumor necrosis factor-alpha following subarachnoid hemorrhage. *J. Neurosurg.* 87, 215–220. doi: 10.3171/jns.1997.87.2.0215
- Mikulski, S. M., Costanzi, J. J., Vogelzang, N. J., Mccachren, S., Taub, R. N., Chun, H., et al. (2002). Phase II trial of a single weekly intravenous dose of ranpirinase in patients with unresectable malignant mesothelioma. *J. Clin. Oncol.* 20, 274–281. doi: 10.1200/JCO.2002.20.1.274
- Niemiec, M. J., De Samber, B., Garrovoet, J., Vergucht, E., Vekemans, B., De Rycke, R., et al. (2015). Trace element landscape of resting and activated human neutrophils on the sub-micrometer level. *Metalomics* 7, 996–1010. doi: 10.1039/C4MT00346B
- Ondracek, A., Hofbauer, T., Wurm, R., Arfsten, H., Seidl, V., Früh, A., et al. (2020). Imbalance between plasma double-stranded DNA and deoxyribonuclease activity predicts mortality after out-of-hospital cardiac arrest. *Resuscitation* 151, 26–32. doi: 10.1016/j.resuscitation.2020.03.006
- Papayannopoulos, V. (2018). Neutrophil extracellular traps in immunity and disease. *Nat. Rev. Immunol.* 18, 134–147. doi: 10.1038/nri.2017.105
- Peterson, J. W., Kwun, B. D., Hackett, J. D., and Zervas, N. T. (1990). The role of inflammation in experimental cerebral vasospasm. *J. Neurosurg.* 72, 767–774. doi: 10.3171/jns.1990.72.5.0767
- Preissner, K. T., Fischer, S., and Deindl, E. (2020). Extracellular RNA as a versatile DAMP and alarm signal that influences leukocyte recruitment in inflammation and infection. *Front. Cell Dev. Biol.* 8:619221. doi: 10.3389/fcell.2020.619221
- Provencio, J. J., Fu, X., Siu, A., Rasmussen, P. A., Hazen, S. L., and Ransohoff, R. M. (2010). CSF neutrophils are implicated in the development of vasospasm in subarachnoid hemorrhage. *Neurocrit. Care* 12, 244–251. doi: 10.1007/s12028-009-9308-7
- Rinkel, G. J., Djibuti, M., Algra, A., and Van Gijn, J. (1998). Prevalence and risk of rupture of intracranial aneurysms: a systematic review. *Stroke* 29, 251–256. doi: 10.1161/01.STR.29.1.251
- Schertz, M., Mehdaoui, H., Hamlat, A., Piotin, M., Banydeen, R., and Mejdoubi, M. (2016). Incidence and mortality of spontaneous subarachnoid hemorrhage in Martinique. *PLoS One* 11:e0155945. doi: 10.1371/journal.pone.0155945
- Schneider, U. C., Davids, A. M., Brandenburg, S., Muller, A., Elke, A., Magrini, S., et al. (2015). Microglia inflict delayed brain injury after subarachnoid hemorrhage. *Acta Neuropathol.* 130, 215–231. doi: 10.1007/s00401-015-1440-1
- Shea, A. M., Reed, S. D., Curtis, L. H., Alexander, M. J., Villani, J. J., and Schulman, K. A. (2007). Characteristics of nontraumatic subarachnoid hemorrhage in the United States in 2003. *Neurosurgery* 61, 1131–1138. doi: 10.1227/01.neu.0000306090.30517.ae
- Sheehan, J. P., Polin, R. S., Sheehan, J. M., Baskaya, M. K., and Kassell, N. F. (1999). Factors associated with hydrocephalus after aneurysmal subarachnoid hemorrhage. *Neurosurgery* 45, 1120–1127. doi: 10.1097/00006123-199911000-00021
- Squiquera, L., Taxman, D. J., Brendle, S. A., Torres, R., Sulley, J., Hodge, T., et al. (2017). Ranpirinase eradicates human papillomavirus in cultured cells and heals anogenital warts in a phase I study. *Antivir. Ther.* 22, 247–255. doi: 10.3851/IMP3133
- Tielking, K., Fischer, S., Preissner, K. T., Vajkoczy, P., and Xu, R. (2019). Extracellular RNA in central nervous system pathologies. *Front. Mol. Neurosci.* 12:254. doi: 10.3389/fnmol.2019.00254
- Van Lieshout, J. H., Dibue-Adjei, M., Cornelius, J. F., Slotty, P. J., Schneider, T., Restin, T., et al. (2018). An introduction to the pathophysiology of aneurysmal subarachnoid hemorrhage. *Neurosurg. Rev.* 41, 917–930. doi: 10.1007/s10143-017-0827-y
- Walberer, M., Tschernatsch, M., Fischer, S., Ritschel, N., Volk, K., Friedrich, C., et al. (2009). RNase therapy assessed by magnetic resonance imaging reduces cerebral edema and infarction size in acute stroke. *Curr. Neurovasc. Res.* 6, 12–19. doi: 10.2174/156720209787466037
- Wang, Y., Li, M., Stadler, S., Correll, S., Li, P., Wang, D., et al. (2009). Histone hypercitrullination mediates chromatin decondensation and neutrophil extracellular trap formation. *J. Cell Biol.* 184, 205–213. doi: 10.1083/jcb.200806072
- Zeng, H., Fu, X., Cai, J., Sun, C., Yu, M., Peng, Y., et al. (2021). Neutrophil extracellular traps may be a potential target for treating early brain injury in subarachnoid hemorrhage. *Transl. Stroke Res.* doi: 10.1007/s12975-021-00909-1 [Epub ahead of print]
- Zhang, Z., Fang, Y., Lenahan, C., and Chen, S. (2020). The role of immune inflammation in aneurysmal subarachnoid hemorrhage. *Exp. Neurol.* 336:113535. doi: 10.1016/j.expneurol.2020.113535

Conflict of Interest: The authors declare that the research was conducted in the absence of any commercial or financial relationships that could be construed as a potential conflict of interest.

Publisher's Note: All claims expressed in this article are solely those of the authors and do not necessarily represent those of their affiliated organizations, or those of the publisher, the editors and the reviewers. Any product that may be evaluated in this article, or claim that may be made by its manufacturer, is not guaranteed or endorsed by the publisher.

Copyright © 2021 Früh, Tielking, Schoknecht, Liu, Schneider, Fischer, Vajkoczy and Xu. This is an open-access article distributed under the terms of the Creative Commons Attribution License (CC BY). The use, distribution or reproduction in other forums is permitted, provided the original author(s) and the copyright owner(s) are credited and that the original publication in this journal is cited, in accordance with accepted academic practice. No use, distribution or reproduction is permitted which does not comply with these terms.